Human Rhesus-associated glycoprotein mediates facilitated transport of NH_3 into red blood cells

Pierre Ripoche*, Olivier Bertrand*, Pierre Gane*, Connie Birkenmeier†, Yves Colin*, and Jean-Pierre Cartron*‡

*Institut National de la Santé et de la Recherche Médicale Unite 76, and Institut National de la Transfusion Sanguine, 6 Rue Alexandre Cabanel, 75015 Paris, France; and †The Jackson Laboratory, Bar Harbor, ME 04609

Edited by Joseph F. Hoffman, Yale University School of Medicine, New Haven, CT, and approved October 26, 2004 (received for review May 25, 2004)

Rhesus (Rh) antigens are carried by a membrane complex that includes Rh proteins (D and CcEe), Rh-associated glycoproteins (RhAG), and accessory chains (LW and CD47) associated by noncovalent bonds. In heterologous expression systems, RhAG and its kidney orthologs function as ammonium transporters. In red blood cells (RBCs), it is generally accepted that NH_3 permeates by membrane lipid diffusion. We have revisited these issues by studying RBC and ghosts from human and mouse genetic variants with defects of proteins that comprise the Rh complex. In both normal and mutant cells, stopped-flow analyses of intracellular pH changes in the presence of inwardly directed methylammonium ($CH_3NH_3^+ + CH_3NH_2$) or ammonium ($NH_4^+ + NH_3$) gradients showed a rapid alkalinization phase. Cells from human and mouse variants exhibited a decrease in their kinetic rate constants that was strictly correlated to the degree of reduction of their RhAG/Rhag expression level. Rate constants were not affected by a reduction of Rh, CD47, or LW. CH_3NH_2/NH_3 transport was characterized by (*i*) a sensitivity to mercurials that is reversible by 2-mercaptoethanol and (*ii*) a reduction of alkalinization rate constants after bromelain digestion, which cleaves RhAG. The results show that RhAG facilitates CH_3NH_2/NH_3 movement across the RBC membrane and represents a potential example of a gas channel in mammalian cells. In RBCs, RhAG may transport NH_3 to detoxifying organs, like kidney and liver, and together with nonerythroid tissue orthologs may contribute to the regulation of the systemic acid–base balance.

ammonium | mouse mutants | Rhesus deficiency

Rhesus (Rh) is a clinically significant blood group system in transfusion medicine (1). Rh blood group antigens are defined by a complex association of membrane polypeptides that includes the nonglycosylated Rh proteins (carriers of RhD and RhCcEe antigens) and Rh-associated glycoprotein (RhAG), which is strictly required for cell-surface expression of Rh antigens (2, 3). In red blood cells (RBCs), the core of the Rh complex may be a tetramer composed of two Rh and two RhAG subunits, to which accessory chains (CD47, LW, and GPB) are associated by noncovalent linkages (2, 4).

The Rh_{null} phenotype is an inherited condition in which various Rh antigen deficiencies result in a clinical syndrome characterized by a hemolytic anemia of varying severity, with abnormalities of the red cell shape (stomato-spherocytosis), cation transport, and membrane phospholipid organization (2, 5). Rh_{null} disease is caused by several different mutations that occur in either the *RHAG* or *RH* loci on chromosomes 6p12-p21 and 1p34-p36, respectively. The Rh complex is missing or severely reduced in RBCs from Rh_{null} individuals without alteration of the genes encoding the accessory chains (2, 5). Because of a variable expressivity, some mutations of the *RHAG* gene result in the total lack of RhAG (and Rh protein), defining the Rh_{null} of the regulator type, but others result in weak RhAG (and Rh protein) levels, defining the Rh_{mod} phenotype (5). Mutations of the *RH* gene resulting in the total lack of Rh protein and only a reduced expression of RhAG (20% of normal) define Rh_{null} as the amorph type. Accordingly, primary defects of either RhAG or Rh protein result in defective cell surface expression and/or transport of the whole Rh complex.

The murine mutations normoblastosis ($Ank1^{nb}$) and spherocytosis ($Spna1^{sph}$) disrupt the RBC spectrin-based cytoskeleton through deficiencies of ankyrin and α-spectrin, respectively. In addition to the well described band 3-ankyrin–protein 4.2 and glycophorin C–protein 4.1–p55 complexes (6), the Rh complex represents a major interaction site between the membrane lipid bilayer and the spectrin-based cytoskeleton. Indeed, recent studies of the erythroid ankyrin-deficient normoblastosis mice and analysis with the yeast two-hybrid system have shown that Ank1 may interact directly with the C-terminal cytoplasmic domains of Rh protein and RhAG (7). Interestingly, in humans this interaction was abolished by a mutation found in an Rh_{null} patient (7).

The first indication of the biological role of Rh proteins came from the discovery of a significant homology, particularly to RhAG, with the methylammonium (MA) permease/ammonium transporter (Mep/Amt) superfamily of ammonium transporters present from bacteria to yeast but absent in vertebrates (8). This discovery was followed by the characterization of two nonerythroid orthologs, RhBG and RhCG (9, 10), and the identification of paralogs in a variety of living species, thereby suggesting the conservation of some critical function (reviewed in ref. 11). Moreover, when expressed in Mep/Amt-deficient yeast, RhAG and RhCG function as bidirectional ammonium transporters (12). Recently, functional studies of Rh glycoproteins in *Xenopus laevis* oocytes were performed but yielded discordant results. Some studies suggested that RhAG-mediated uptake of MA in oocytes was an electroneutral NH_4^+/H^+ exchange (13), whereas electrophysiological studies in voltage-clamped RhBG- and RhCG-expressing oocytes suggested that transport is (14, 15) or is not (16) electrogenic. It was also speculated that Rh and Mep/Amt proteins might be facilitators for NH_3 gas transport (17).

In physiological systems, such as RBCs, it is generally accepted that NH_3 permeates through membrane lipid diffusion (18–20). The purpose of the present study is to revisit these findings by studying the ammonium transport in RBCs from human and mouse genetic variants with various defects of proteins that comprise or interact with the Rh complex. Accordingly, stopped-flow analysis of kinetic rate constants of intracellular pH (pH_i) changes of resealed ghosts in the presence of MA or ammonium gradients as well as mercurial inhibition and protease cleavage studies were performed. The results indicate that RhAG facilitates CH_3NH_2/NH_3 movement across the red cell membrane.

Materials and Methods

Blood Samples. Four Rh_{null} patients of the regulator type [P1(TB), P2(YT), P3(AL), and P4(AC)], one Rh_{mod} patient [P5(CB)], and

This paper was submitted directly (Track II) to the PNAS office.

Abbreviations: Rh, Rhesus; RhAG, Rh-associated glycoprotein; RBC, red blood cell; MA, methylammonium; pH_i, intracellular pH.

‡To whom correspondence should be addressed. E-mail: cartron@idf.inserm.fr.

www.pnas.org/cgi/doi/10.1073/pnas.0403704101

one Rh_{null} patient of the amorph type [P6(DR)] have been described (2, 5). Control RBCs from RhD-positive, RhD-negative, and LW_{null} individuals [P7(Big) and P8(Mil)] were provided by the Centre de Référence pour les Groupes Sanguins (Paris). RBCs from two individuals [P9(Sar) and P10(Fer)] of the $AQP1_{null}$ phenotype lacking AQP1 (also called CO_{null} because AQP1 carries Colton antigens) have been described (21, 22). A blood sample from a 4.2-deficient patient [P11(Rem)] was provided by O. Agulles (Etablissement Français du Sang, Nancy, France). RBCs from mouse models of hereditary hemolytic anemia, normoblastosis (*nb/nb*) (ankyrin-deficient) and spherocytosis (*sph/sph*) (spectrin-deficient), and from wild-type mice (WBB6F1, C57BL/6J) were from The Jackson Laboratory. Before analysis, cryopreserved or fresh RBCs were washed twice with PBS.

Flow Cytometry Analysis. Indirect immunofluorescence of human and mouse RBCs for cell-surface or intracellular epitope analysis was performed with a FACScalibur flow cytometer (Pharmingen) by using the following monoclonal antibodies: mouse anti-human Rh protein BRIC69 (D. Anstee, International Blood Group Reference Laboratory, Bristol, U.K.), mouse anti-human CD47 (clone 3E12, Bioatlantique, Nantes, France), rat anti-mouse CD47 (clone miap 301, Pharmingen), mouse anti-LW BS46 (H. H. Sonneborn, Offenbach, Germany), human anti-Band 3 HIRO-58/Di^b (M. Uchikawa, Japanese Red Cross Central Blood Center, Tokyo); mouse anti-AQP1 (clone 1/A5F6, Serotec, Cergy, France), and rabbit polyclonal antibodies to human Rh protein (MPC8) and mouse Rhag (mC-TRhAG). The antibodies were used at saturating conditions as described in refs. 3, 7, and 23. In control studies, a human anti-Colton a antigen (Centre de Référence pour les Groupes Sanguins, Paris) and a rabbit polyclonal antibody to AQP3 protein were used with intact and fixed permeabilized RBCs as described in refs. 24 and 25.

RBC Ghost Preparation. All preparation steps, except resealing (37°C), were carried out at 4°C, and assays were performed the same day (26). One volume of blood was washed three times in resealing buffer (140 mM NaCl/2.5 mM KCl/10 mM Hepes/NaOH, pH 7.4) and resuspended in 80 volumes of hypotonic lysis buffer (7 mM NaCl/10 mM Hepes/NaOH, pH 7.4) for 40 min on ice folllowed by resealing in resealing buffer containing 1 mM $MgSO_4$ and 0.15 mM pyranine, the fluorescent pH-sensitive dye (1-hydroxypyrene-3,6,8-trisulfonic acid, Sigma–Aldrich) at 37°C for 1 hr. After three washes in resealing buffer, ghosts were equilibrated in buffer A (130 mM NaCl/5 mM KCl/10 mM Hepes/NaOH, pH 7.0) and kept on ice before assays.

pH_i Determination by Stopped-Flow Analysis. Ammonium or MA (ammonium and MA refer to the sum of protonated and unprotonated forms) transport was measured in isoosmotic conditions. Membrane ghosts equilibrated in buffer A containing 5 mM *p*-xylene-bis(*N*-pyridinium bromide) (Sigma), a fluorescence quencher of external pyranine, were mixed with an equal volume of buffer B (65 mM NaCl/5 mM KCl/65 mM NH_4Cl or MA chloride/10 mM Hepes/NaOH, pH 7.0), generating an inwardly directed 32.5 milliequivalent gradient. In preliminary experiments, pH_i changes were measured with a stopped-flow instrument (SFM3, Biologic, Grenoble, France) that was modified by addition of the titrator device (Biologic), which consists of replacing the 30-μl cuvette (see below) with a thermostated (15°C) and vortex-mixed cuvette (4 ml), allowing the use of the equipment as an ordinary spectrofluorometer. The excitation wavelength was 460 nm, and the emitted light was filtered with a 520-nm cut-on filter. The pH-dependent fluorescence changes were followed and analyzed, because a fluorescence increase corresponded to a pH elevation and a fluorescence decrease corresponded to a pH reduction (27). Over the pH range used (7.0–7.8), the relative fluorescence of the dye was proportional to pH, as determined by titration on ghosts incubated in 2 ml of buffer A containing 5 mM *p*-xylene-bis(*N*-pyridinium bromide) and 5 μM nigericin (Sigma) and submitted to pH change by step additions of 2 μl of KOH (1 M). Subsequently, ghost alkalinization and acidification kinetics were performed in the stopped-flow mode (30-μl FC-15 cuvette; dead time, 7.8 ms). Preliminary experiments showed that ammonium transport was similar for ghosts prepared from fresh and cryopreserved RBCs. Data from five to eight time courses were averaged, and the alkalinization phase was fitted to a single exponential function by using the Simplex procedure of the BIOKINE software (Biologic) to calculate kinetic rate constants, k, in s^{-1}. In some experiments, apparent permeabilities (P') were determined without unstirred layers correction according to Priver *et al*. (28) by using the following equation:

$$P' = (\Delta pH_{max})\cdot(BC)\cdot(V/SA)/\Delta C\cdot t,$$

where ΔpH_{max} is the maximum pH change value, BC is the buffer capacity, V/SA is the volume-to-surface-area ratio (in cm) of ghosts, ΔC is the MA/ammonium gradient (mM), and $t = 1/k$ (s), which is the reciprocal of the exponential kinetic rate constant k.

Membrane ghosts are crenated spheres in isotonic solution (29). Determination of ghost diameter by light and confocal microscopy confirmed their spheric shape and that ghosts are smaller than intact RBCs. When ghosts from normal and human variant RBCs were compared, we found no significant difference (4.95 ± 0.2 versus 5.07 ± 0.38 μm). The volume calculated from the measured mean diameter corresponds to a sphere of $\approx 7 \times 10^{-14}$ liter, as expected (30). The buffer capacity of ghosts in buffer A containing 5 mM *p*-xylene-bis(*N*-pyridinium bromide) was measured by a single addition of 20 mM acetate as in ref. 27, but with the stopped-flow mode. The mean value was within the same range for normal and variant ghosts (82.57 ± 9.83 versus 82.18 ± 3.71 mM per pH unit). In some experiments, ghosts were incubated for 5 min at 15°C in the presence of 0.1 mM $HgCl_2$ before the application of the MA gradient. In other experiments, ghosts were prepared from protease-treated RBCs that were obtained by incubating washed RBCs (10% hematocrit) for 30 min at 37°C in the presence or absence of 3 mg/ml bromelain (product no. B4882, Sigma) in PBS. Then, cysteine proteinase inhibitor transepoxysuccinyl-L-leucylamido-(-4-guanidino)butane (E-64, Calbiochem) was added to a 10 μM final concentration, and RBCs were washed three times at 4°C in PBS containing 10 μM E64.

Water and Glycerol Permeabilities and Western Blot Analysis. Water and glycerol osmotic permeabilities were determined by RBC volume change analysis in the stopped-flow spectrophotometer by measuring 90° scattered-light intensity with 600-nm excitation light, as described in ref. 31. Western blot analyses of native and protease-treated ghosts were performed with a murine monoclonal anti-RhAG (clone LA 18-18, gift from A. van dem Borne, University of Amsterdam, Amsterdam), the reactivity of which depends on the presence of the carbohydrate moiety, and with rabbit antisera against the C-ter of human RhAG (anti-C-ter) and MPC8 (12, 23).

Results and Discussion

CH_3NH_2/NH_3 Transport in Normal RBC Ghosts. Studies of ammonium permeability by ^{14}N and ^{15}N saturation transfer NMR spectroscopy have demonstrated that NH_3 very rapidly enters RBCs by passive lipid diffusion (20). To further investigate this question, we have studied RBC and ghosts from human and mouse genetic

Table 1. Antigen and protein expression of human RBCs

Membrane protein	Control	Variants					
	RhD-positive ($n = 5$)	Rh_{null} regulator of P1–P4	Rh_{mod} of P5	Rh_{null} amorph of P6	LW_{null} of P7/P8	4.2_{null}* of P11	$AQP1_{null}$ of P9/P10
Rh	126 ± 10	0	7.6	0.1	90/100	112	131/136
RhAG	81 ± 7	<0.2	8.9	17.6	65/75	108	85/95
CD47	17 ± 1	1.9 ± 0.2	3	2.3	13/15	4.1	17/16
LW	3 ± 1	0	0	0	0/0	4	n.t.
Band 3	2,129 ± 60	2,076 ± 46	1,987	2,139	1,927/1,762	1,853	2,029
AQP1	298 ± 15	270 ± 24	243	318	350/380	297	<0.2
AQP3	172 ± 10	151 ± 26	152	169	133/157	199	119

Values indicate the copy number of membrane protein per red cell ($\times 10^{-3}$), except for Band 3, AQP1 (anti-Colton a antigen), and AQP3, which were measured as mean fluorescence intensity. n.t., not tested.
*Only a single patient was tested.

variants with defects of proteins that comprise the Rh complex. Because ammonium is a weak base ($pK_a = 9.56$ at 15°C), cell uptake results in pH_i changes, either alkalinization or acidification, depending on whether the neutral form (NH_3) or charged form (NH_4^+) is taken up. Because of the high buffer capacity of RBCs, pH_i changes were determined on membrane ghosts resealed on a 10 mM Hepes buffer (pH 7.0) containing pyranine as a fluorescent pH-sensitive dye. Because all ghosts preparations, including those from controls from human variant RBCs analyzed below, exhibited a similar size and buffer capacity (see *Materials and Methods*), the kinetic rate constants of CH_3NH_2/NH_3 influx measured in transport studies strictly reflected differences in permeabilities to CH_3NH_2/NH_3.

By using ghosts from control RhD-positive RBCs with normal Rh, RhAG, LW, and CD47 expression (Table 1) submitted to a 32.5 mM inwardly directed MA or ammonium gradient (pH 7.0) in isoosmotic conditions, we found that the fluorescence intensity curve exhibited a biphasic response, consisting first of a rapid phase of alkalinization ($\Delta pH \approx 0.5$ unit), followed by a slow acidification phase to return to external pH (pH_0) of the incubation medium (Fig. 1*A*). The alkalinization can be accounted for by the uptake of CH_3NH_2 or NH_3, thereby trapping protons within the cells until the equilibrium values of these neutral forms were reached (20). The kinetic rate constant of alkalinization of ghosts from RhD-positive cells (Fig. 1*B*) was $0.95 \pm 0.1\ s^{-1}$ for CH_3NH_2 and $4.95 \pm 0.28\ s^{-1}$ for NH_3, and there was no significant difference between ghosts from RhD-positive and RhD-negative RBCs. RhD-positive and RhD-negative RBCs exhibiting normal levels of RhAG, LW, CD47, and RhCE proteins but differing by the presence or absence of the RhD protein, suggests that, by itself, the RhD protein has no significant effect on CH_3NH_2/NH_3 transport. From these data, the calculated apparent permeabilities (P′) of RhD-positive ghosts for CH_3NH_2 and NH_3 at 15°C are $0.88 \pm 0.09\ 10^{-4}$ and $4.46 \pm 0.25\ 10^{-4}$ cm·s^{-1}, respectively, without the correction of the unstirred layers (Table 2). A value in the same range has been published for NH_3 permeability of RBCs at 21°C (20). Although most experiments were done with a 32.5 mM gradient, some were also performed with 2.5–40 mM MA (pH 7.0) gradients, and we found a linear relationship with fluorescence variation (data not shown).

The phase of slow acidification after the alkalinization step corresponds to a return to pH_0, which is a complex process, because the ghost membrane carries several transporters, such as Band 3 and specific or nonspecific ammonium/MA transporter(s), including the Na^+/H^+ antiport, that could participate in pH regulation. This process was not investigated further. Because the acidification phase is 25 or 45 times slower than the alkalinization phase (as estimated by $t_{1/2}$ values for CH_3NH_2 and NH_3, respectively), we assume that it does not significantly interfere with the calculation of first-phase rate constants.

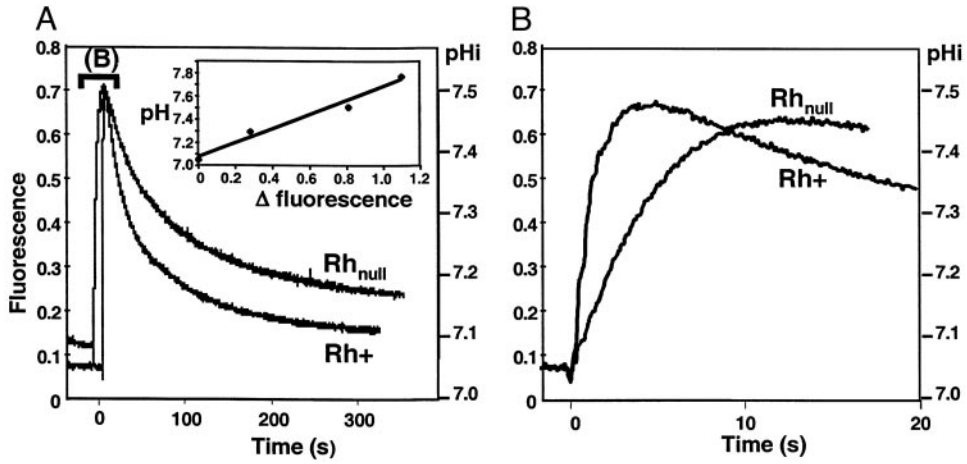

Fig. 1. Time course of fluorescence and pH_i changes in ghosts. (*A*) Ghosts from RhD-positive (Rh+) and Rh_{null} regulator (P1) were submitted to a 32.5 mM MA inwardly directed gradient (pH 7.0) at 15°C, and pH_i changes were followed by fluorescence change of a pH-sensitive dye in the stopped-flow spectrofluorometer by using the titrator device (see *Materials and Methods*). The response was biphasic. Experiments were repeated three times with different Rh_{null} of the regulator type (P2, P3, and P4) and yielded the same results. (*Insert*) Over the pH range used (7.0–7.8), the relative fluorescence of the dye was proportional to pH. (*B*) Expanded scale of the rapid alkalinization phase.

Table 2. Rate constants and permeability to CH_3NH_2/NH_3 of human RBC ghosts

	Controls		Variants				
Substrate	RhD-positive ($n = 3$)	RhD-negative ($n = 3$)	Rh_{null} regulator of P1–P4	Rh_{mod} of P5	Rh_{null} amorph of P6	LW_{null} of P7/P8	4.2_{null} of P11
CH_3NH_2							
k, s^{-1}	0.95 ± 0.1	0.81 ± 0.03	0.14 ± 0.03*	0.26	0.38	0.8/0.8	0.74
P', $cm \cdot s^{-1}$	0.88 ± 0.09	0.71 ± 0.03	0.12 ± 0.03*	0.23	0.36	0.8/0.7	0.68
NH_3							
k, s^{-1}	4.95 ± 0.28	5.4 ± 0.28	2.48 ± 0.09*	2.6	2.9	3.9/4.1	4.56
P', $cm \cdot s^{-1}$	4.46 ± 0.25	3.91 ± 0.21	2.54 ± 0.08*	2.63	2.53	4.1/4.3	4.11

Figures indicate alkalinization rate constants (k) and permeability ($P' \times 10^{-4}$) to CH_3NH_2/NH_3 of ghosts submitted to 32.5 mM MA or ammonium gradient. *, $P < 0.001$ versus RhD-positive and RhD-negative.

CH_3NH_2/NH_3 Transport of Ghosts from Human Variants. We next determined pH_i changes of ghosts from Rh_{null} cells of the regulatory type (no Rh/RhAG/LW; low CD47) (Table 1), and we found also a biphasic response (Fig. 1). However, the rate constants of alkalinization were much slower ($0.14 \pm 0.03\ s^{-1}$) compared with control RBCs, because of a 6-fold reduction of apparent permeability to CH_3NH_2 (Table 2). Rh_{mod} and Rh_{null} (amorph) ghosts that express only 10% and 20% of RhAG, respectively (Table 1), exhibited intermediate values (Fig. 2*A* and Table 2), suggesting that CH_3NH_2 transport was correlated to RhAG expression level. pH_i changes were faster in the presence of the NH_4Cl gradient at pH 7.0 (Fig. 2*B*), but there was still an ≈2-fold reduction of alkalinization rate constants and P′ values for Rh_{null} regulators compared with controls, again with Rh_{mod} and Rh_{null} (amorph) exhibiting intermediate values (Table 2). The fact that the rates change in the same-sized ghosts with or without Rh proteins indicates that the unstirred layers do not play a significant role. Therefore, although a "basal" CH_3NH_2/NH_3 entry occurs by lipid diffusion in Rh_{null} cells, our data strongly suggest that RhAG may accelerate this process. As shown in Table 2, we also found a normal alkalinization rate constant of ghosts from LW_{null} RBCs (normal Rh/RhAG/CD47; no LW) (Table 1), indicating no role of LW in CH_3NH_2/NH_3 transport. In addition, the alkalinization rate constant of 4.2_{null} ghosts, which have a severe reduction of CD47 but normal levels of Rh, RhAG, and LW (Table 1) (23, 32), was only slightly lower in the single patient (P11) investigated ($0.74\ s^{-1}$ for CH_3NH_2), indicating that CD47 does not play a significant role. We found, however, that $AQP1_{null}$ (CO_{null}) ghosts with a normal content of RhAG (Table 1) showed a small but significant ($P < 0.01$) reduction of CH_3NH_2 transport ($k = 0.51\ s^{-1}$ for P9 and $0.59\ s^{-1}$ for P10 versus $k = 0.95 \pm 0.1\ s^{-1}$ for control RBCs), suggesting that AQP1 might partly contribute to NH_3 transport, as suggested in ref. 33.

The differences of alkalinization rate constants and permeabilities seen between CH_3NH_2 and NH_3 with Rh control samples (≈5-fold) might reflect the different molecular structure of these substrates (Table 2). These differences are even larger with Rh_{null} samples (≈20-fold), in which the transport is most likely limited to lipid diffusion. Interestingly, 4.2_{null} ghosts, which derived from RBCs with the same morphological characteristics as Rh_{null} cells (34), have a normal RhAG protein content (Table 1) and exhibit a transport activity virtually identical to that of controls (Fig. 2*A* and Table 2). Moreover,

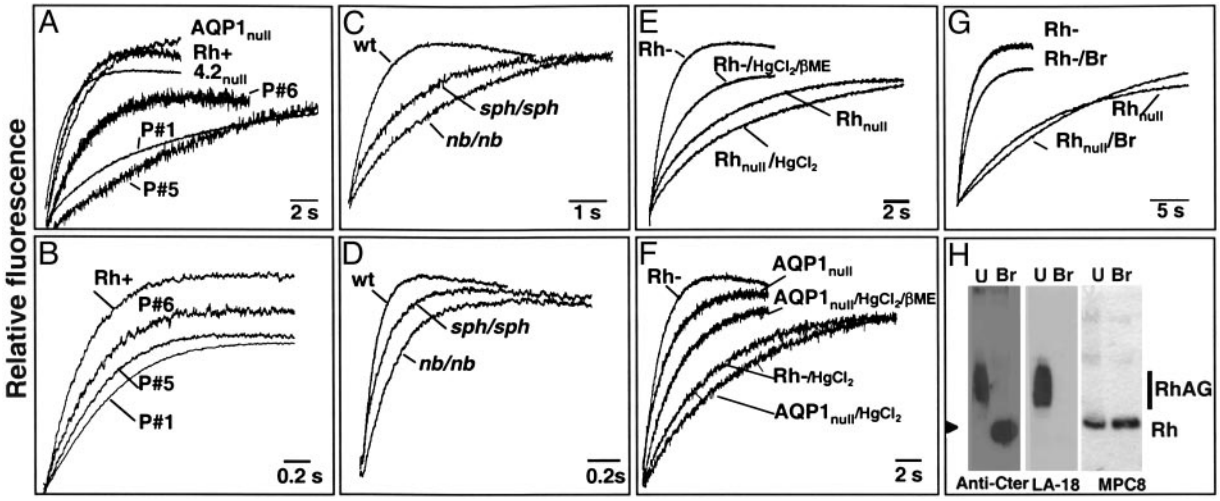

Fig. 2. CH_3NH_2/NH_3 transport in ghosts from human and mouse variants. (*A–G*) Time course of fluorescence change of human (*A*, *B*, and *E–G*) and murine (*C* and *D*) ghosts subjected to a 32.5 mM MA (*A*, *C*, and *E–G*) or ammonium (*B* and *D*) inwardly directed gradient (pH 7.0) at 15°C were followed by stopped-flow analysis (see *Materials and Methods*). Only the rapid initial alkalinization phase is shown. (*A* and *B*) Human samples: RhD-positive (Rh+), Rh_{null} regulator (P1), Rh_{mod} (P5), Rh_{null} amorph (P6), 4.2_{null} (P11), and $AQP1_{null}$ (P9). (*C* and *D*) Mouse samples: wild type (wt), *nb/nb*, and *sph/sph*. (*E* and *F*) Thiol sensitivity. Ghosts from RBCs were preincubated with 0.1 mM $HgCl_2$, followed by a treatment with or without 5 mM 2-mercaptoethanol (β-ME). (*E*) Effect on RhD-negative (Rh−) and Rh_{null} (P1) ghosts and reversibility by 2-mercaptoethanol. (*F*) Effect on $AQP1_{null}$ (P9) ghosts. (*G* and *H*) Effect of proteolytic degradation. (*G*) MA transport was reduced in Rh-negative but not Rh_{null} (P1) ghosts prepared from RBCs digested with bromelain (Br). (*H*) Western blot analysis of ghosts prepared from untreated (U) or bromelain-digested (Br) Rh-negative RBCs. Blots were immunostained with a rabbit serum against human RhAG (anti-C-ter), the mouse monoclonal LA18-18 (anti-human RhAG), and MPC8 (anti-human Rh protein). The arrowhead indicates digested RhAG product.

Table 3. Volume change rate constants of human and mouse RBCs

	Human RBCs					Mouse RBCs			
Solute	RhD-positive ($n = 3$)	RhD-negative ($n = 1$)	Rh_{null} regulator	Rh_{mod}	Rh_{null} amorph	WBB6F1 ($n = 6$)	C57BL/6J ($n = 6$)	*nb/nb* ($n = 5$)	*sph/sph* ($n = 7$)
Sucrose	3.29 ± 0.2	3.14	3.67 ± 0.46 (P1–P4)	3.29 (P5)	2.73 (P6)	7.73 ± 0.27	6.67 ± 0.27	5.15 ± 0.23*	3.51 ± 0.09*
Glycerol	0.14 ± 0.016	n.t.	0.14 ± 0.01 (P1 and P2)	n.t.	n.t.	0.091 ± 0.01	0.062 ± 0.002	0.1 ± 0.007	0.07 ± 0.003

Values indicate volume change rate constants of RBCs submitted to 100 mM sucrose or 150 mM glycerol gradients. Rate constants (in s^{-1}) were calculated from shrinkage for water movement and swelling for glycerol uptake. n.t., not tested. *, $P < 0.001$.

Rh_{null} of the regulator and amorph types also have the same morphological characteristics (2), but they exhibit different rate constant values (Table 2) that follow their difference in RhAG content (Table 1). As a further test of whether cell volume variation affects the comparative analysis of rate constants, RBC permeabilities to water and glycerol under hyperosmotic conditions (100 and 150 mM sucrose and glycerol gradients, respectively) were determined. No significant differences were observed between control and Rh-variant cells (Table 3*A*), except for the water permeability of $AQP1_{null}$ cells that, as expected (21), was severely reduced (data not shown).

Our results show that Rh_{null} cells exhibit reduced permeabilities to CH_3NH_2 and NH_3 that may be related to their protein defects. However, it is known that the membrane lipid composition and the leaflet bilayer asymmetry may affect NH_3 permeability (35, 36). The composition and content of red cell lipids and phospholipids in Rh_{null} RBCs has been examined in only a few cases and was found to be normal (37, 38). However, there is an abnormal membrane distribution of phosphatidylethanolamine and an enhanced transbilayer movement of phosphatidylcholine (39). The membrane fluidity of Rh_{null} cells is poorly documented but has been found to be either normal (40, 41) or slightly increased (42), suggesting that such small variations cannot account for the large reduction of alkalinization rate constants of Rh_{null} ghosts (Table 2).

Our results showing that RhAG accelerates NH_3 import contradict the conclusion of a recent report based on a method inappropriate to measure fast kinetics (43).

CH_3NH_2/NH_3 Transport of Ghosts from Mutant Mice. Further studies were carried out by using mouse models of hereditary hemolytic anemia. These mice have primary defects in Ank1 (*nb/nb*) (44) or α-spectrin (*sph/sph*) (45). RBCs from *nb/nb* mice exhibit a sharp reduction of Rh and Rhag proteins but normal levels of CD47 (7), which is also true for RBCs from *sph/sph* mice (Table 4). Accordingly, we hypothesized that, similarly to Rh_{null} cells, these cells would exhibit reduced CH_3NH_2 or NH_3 transport activity. Indeed, the alkalinization rate constants in the presence of a MA gradient (pH 7.0) were high in wild type (1.55 s^{-1}) and much lower, although correlated to their respective level of Rhag protein, in *nb/nb* (0.38 s^{-1}) and *sph/sph* (0.66 s^{-1}) mice (Fig. 2*C* and Table 4). The rate constants were much faster with an ammonium gradient at pH 7.0 (Fig. 2*D*), but there was still a difference between wild type (12.8 s^{-1}) and mutant mice (7.6 and 5.5 s^{-1}). These results support the view that the Rhag protein plays a role in CH_3NH_2/NH_3 transport of mouse RBCs. In control experiments, although mouse RBCs lack AQP3 (25, 46), we found no significant differences in the passive lipid diffusion of glycerol. However, the water permeability of mutant mice RBCs was reduced compared with wild type (Table 3) but was correlated to an apparent lower level of AQP1 (Table 4).

Table 4. Antigen and protein expression of mouse RBCs

	Controls		Variants	
Membrane component	WBB6F1 ($n = 3$)	C57BL/6J ($n = 3$)	*nb/nb* ($n = 3$)	*sph/sph* ($n = 3$)
Rh	505 ± 15	n.t.	31 ± 1	181 ± 4
RhAG	272 ± 4	264 ± 18	7 ± 2	117 ± 5
CD47	104 ± 2	103 ± 2	104 ± 5	111 ± 2
Band 3	2,200 ± 30	2,139 ± 33	773 ± 40	1,088 ± 8
AQP1*	504 ± 31	519 ± 17	356 ± 20	321 ± 12
AQP3	24 ± 1	30 ± 1	25 ± 1	30 ± 2

Values indicate expression level of membrane components measured as mean fluorescence intensity. n.t., not tested.
*Monoclonal antibody 1/A5F6.

CH_3NH_2/NH_3 Transport Function Is Mediated by a Protein-Dependent Pathway. Altogether, the kinetic studies with human and mouse variants indicate either more rapid diffusion of CH_3NH_2/NH_3 across membrane lipids in normal ghosts or accelerated movement mediated by the presence of RhAG. To provide further evidence for protein-mediated transport, we examined the effect of $HgCl_2$, which is known to interact with thiol groups of proteins on the alkalinization rate constants of ghosts from control RBCs (either RhD-positive or RhD-negative) and from RBCs of the Rh_{null} regulator type. Preincubation of RBCs with 1 mM $HgCl_2$ severely reduced the rate constants of RhD-negative ghosts (and RhD-positive; data not shown) to the value typical of untreated Rh_{null} cells, and this effect was reversible with 5 mM 2-mercaptoethanol (Fig. 2*E*). Moreover, pretreatment of Rh_{null} cells with $HgCl_2$ did not further reduce their transport activity (data not shown), whereas $AQP1_{null}$ ghosts (no AQP1; normal RhAG) (Table 1) behaved as control cells before and after incubation with $HgCl_2$ (and 2-mercaptoethanol treatment) (Fig. 2*F*). As additional proof that permeability to CH_3NH_2/NH_3 is facilitated by a membrane protein, transport experiments were performed with ghosts prepared from protease-digested RBCs. Because bromelain cleaves RhAG and RhD, but not the RhCE protein (47), the experiments were carried out with RhD-negative cells. Ghosts from bromelain-digested RBCs exhibited a significant reduction of the alkalinization rate constant compared with the untreated control (Fig. 2*G*), whereas protease digestion of Rh_{null} (regulator) cells had no effect. Western blot analysis confirmed that RhAG but not the Rh protein of ghosts prepared from enzyme-treated RBCs was cleaved by bromelain (Fig. 2*H*).

Altogether, our results favor a critical role of the RhAG protein in CH_3NH_2/NH_3 transport. Moreover, the results showing that RhAG facilitates CH_3NH_2/NH_3 movement across the red-cell membrane point to RhAG as a potential example of a gas channel in mammalian cells. There are $\approx 2 \times 10^5$ copies of RhAG per RBC and presumably 2 RhAG molecules per Rh complex (2), which leaves us with $\approx 10^5$ copies of functional Rh complexes. From these data and transport studies (Table 2), we tentatively calculate that for a 1 M ammonium gradient (pH 7.0), there is an approximate conductance of 2×10^6 NH_3 molecules per second per Rh complex.

Our results support previous speculation (17) that Rh proteins may facilitate diffusion of NH_3. However, it was also proposed recently that the Rh1 protein paralog of the green alga *Chla-*

mydomonas reinhardtii might be regarded as a gas channel for CO_2, because mutants lacking this protein grow only very slowly when cultured in high CO_2 conditions (48). That Rh proteins might transport NH_3 and/or CO_2 is a possibility that should be further explored (32). Although still a matter of debate (49, 50), current studies suggest that the water channel AQP1 may represent another example of protein permeable to gases, because it also substantially increases the permeability of the membrane to CO_2 (50, 51) and NH_3 (33). Moreover, NtAQP1-related CO_2 permeability in plants plays a physiological role in photosynthesis and stomatal opening, particularly under low CO_2 gradient conditions (52).

Most interestingly, after this article was submitted, Khademi *et al*. (53) resolved the crystallographic structure of the bacterial NH_3 transport channel AmtB and showed by reconstitution into vesicles that AmtB conducts uncharged NH_3, which is fully consistent with our present studies on the RhAG protein.

In RBCs, RhAG may act to carry NH_3 to detoxifying organs, like kidney and liver (12). However, the transport function with regard to the substrate transported may be different according to which cells or tissues are examined and which Rh protein homologue (RhAG, RhBG, or RhCG) is present. These findings should stimulate further investigation of the physiological role of RhAG orthologs in nonerythroid tissues to understand their role in the regulation of systemic acid–base balance. These proteins might also play a role as ammonium/NH_3 sensors in the regulation of various cellular functions, such as ion transports, in response to variations in extracellular ammonium level (54–56).

We thank A. Sentenac and J. M. Verbavatz (Commissariat à l'Energie Atomique/Saclay, Gif sur Yvette, France) for the stopped-flow equipment and Dr. O. Agulles for the 4.2-deficient sample.

1. Mollison, P. L., Engelfriet, C. P. & Contreras, M. (1997) *Blood Transfusion in Clinical Medicine* (Blackwell, London), 10th Ed., pp. 152–184.
2. Cartron, J. P. (1999) *Baillieres Best Pract. Res. Clin. Haematol.* **12,** 655–689.
3. Mouro-Chanteloup, I., D'Ambrosio, A. M., Gane, P., Le Van Kim, C., Raynal, V., Dhermy, D., Cartron, J. P. & Colin, Y. (2002) *Blood* **100,** 1038–1047.
4. Avent, N. D. & Reid, M. E. (2000) *Blood* **95,** 375–387.
5. Huang, C. H., Liu, P. Z. & Cheng, J. G. (2000) *Semin. Hematol.* **37,** 150–165.
6. Lux, S. E. & Palek, J. (1995) in *Blood: Principles and Practice of Hematology*, eds. Handlin, S. E., Lux, S. E. & Stossel, T. P. (Lippincott, Philadelphia), pp. 1701–1818.
7. Nicolas, V., Le Van Kim, C., Gane, P., Birkenmeier, C., Cartron, J. P., Colin, Y. & Mouro-Chanteloup, I. (2003) *J. Biol. Chem.* **278,** 25526–25533.
8. Marini, A. M., Urrestarazu, A., Beauwens, R. & Andre, B. (1997) *Trends Biochem. Sci.* **22,** 460–461.
9. Liu, Z., Chen, Y., Mo, R., Hui, C., Cheng, J. F., Mohandas, N. & Huang, C. H. (2000) *J. Biol. Chem.* **275,** 25641–25651.
10. Liu, Z., Peng, J., Mo, R., Hui, C. & Huang, C. H. (2001) *J. Biol. Chem.* **276,** 1424–1433.
11. Huang, C. H. & Liu, P. Z. (2001) *Blood Cells Mol. Dis.* **27,** 90–101.
12. Marini, A. M., Matassi, G., Raynal, V., Andre, B., Cartron, J. P. & Cherif-Zahar, B. (2000) *Nat. Genet.* **26,** 341–344.
13. Westhoff, C. M., Ferreri-Jacobia, M., Mak, D. O. & Foskett, J. K. (2002) *J. Biol. Chem.* **277,** 12499–12502.
14. Nakhoul, N. L. DeJong, H., Abdulnour-Nakhoul, S. M., Boulpaep, E. L., Hering-Smith, K. & Hamm, L. L. (2004) *Am. J. Renal. Physiol.*, in press.
15. Bakouh, N., Benjelloun, F., Hulin, P., Brouillard, F., Edelman, A., Cherif-Zahar, B. & Planelles, G. (2004) *J. Biol. Chem.* **279,** 15975–15983.
16. Ludewig, U. (2004) *J. Physiol. (Paris)* **559,** 751–759.
17. Soupene, E., Ramirez, R. M. & Kustu, S. (2001) *Mol. Cell. Biol.* **21,** 5733–5741.
18. Klocke, R. A., Andersson, K. K., Rotman, H. H. & Forster, R. E. (1972) *Am. J. Physiol.* **222,** 1004–1013.
19. Aubert, L. & Motais, R. (1975) *J. Physiol. (Paris)* **246,** 159–179.
20. Labotka, R. J., Lundberg, P. & Kuchel, P. W. (1995) *Am. J. Physiol.* **268,** C686–C699.
21. Preston, G. M., Smith, B. L., Zeidel, M. L., Moulds, J. J. & Agre, P. (1994) *Science* **265,** 1585–1587.
22. Chrétien, S., De Figueiredo, M. & Cartron, J. P. (1999) *Blood* **93,** 4021–4022.
23. Mouro-Chanteloup, I., Delaunay, J., Gane, P., Nicolas, V., Johansen, M., Brown, E. J., Peters, L. L., Le Van Kim, C., Cartron, J. P. & Colin, Y. (2003) *Blood* **101,** 338–344.
24. Trinh-Trang-Tan, M. M., Lasbennes, F., Gane, P., Roudier, N., Ripoche, P., Cartron, J. P. & Bailly, P. (2002) *Am. J. Physiol. Renal. Physiol.* **283,** F912–F922.
25. Roudier, N., Ripoche, P., Gane, P., Le Pennec, P. Y., Daniels, G., Cartron, J. P. & Bailly, P. (2002) *J. Biol. Chem.* **277,** 45854–45859.
26. Mohandas, N., Clark, M. R., Health, B. P., Rossi, M., Wolfe, L. C., Lux, S. E. & Shohet, S. B. (1982) *Blood* **59,** 768–774.
27. Damiano, E., Bassilana, M., Rigaud, J. L. & Leblanc, G. (1984) *FEBS Lett.* **166,** 120–124.
28. Priver, N. A., Rabon, E. C. & Zeidel, M. L. (1993) *Biochemistry* **32,** 2459–2468.
29. Sheetz, M. P. & Singer, S. J. (1977) *J. Cell Biol.* **73,** 638–646.
30. Doberstein, S. K., Wiegand, G., Machesky, L. M. & Pollard, T. D. (1995) *Cytometry* **20,** 14–18.
31. Roudier, N., Verbavatz, J. N., Maurel, C., Ripoche, P. & Tacnet, F. (1998) *J. Biol. Chem.* **273,** 8407–8412.
32. Bruce, L. J., Ghosh, S., King, M. J., Layton, D. M., Mawby, W. J., Stewart, G. W., Oldenborg, P. A., Delaunay, J. & Tanner, M. J. (2002) *Blood* **100,** 1878–1885.
33. Nakhoul, N. L., Hering-Smith, K. S., Abdulnour-Nakhoul, S. M. & Hamm, L. L. (2001) *Am. J. Physiol. Renal. Physiol.* **281,** F255–F263.
34. Beauchamp-Nicoud, A., Morle, L., Lutz, H. U., Stammler, P., Agulles, O., Petermann-Khder, R., Iolascon, A., Perrotta, S., Cynober, T., Tchernia, G., *et al*. (2000) *Haematologica* **85,** 19–24.
35. Lande, M. B., Donovan, J. M. & Zeidel, M. L. (1995) *J. Physiol. (Paris)* **106,** 67–84.
36. Hill, W. G., Rivers, R. L. & Zeidel, M. L. (1999) *J. Gen. Physiol.* **114,** 405–414.
37. Sturgeon, P. (1970) *Blood* **36,** 310–320.
38. Ballas, S. K., Clark, M. R., Mohandas, N., Colfer, H. F., Caswell, M. S., Bergren, M. O., Perkins, H. A. & Shohet, S. B. (1984) *Blood* **63,** 1046–1055.
39. Kuypers, F., van Linde-Sibenius-Trip, M., Roelofsen, B., Tanner, M. J. A., Anstee, D. J. & Op Den Kamp, J. A. F. (1984) *Biochem. J.* **221**, 931–934.
40. Smith, J. A., Lucas, F. V., Jr., Martin, A. P, Senhauser, D. A. & Vorbeck, M. L. (1973) *Biochem. Biophys. Res. Commun.* **54,** 1015–1023.
41. Thulborn, K. R., Sawyer, W. H. & Smith, J. A. (1977) *Blood* **50,** 964–965.
42. Dorn-Zachertz, D. & Zimmer, G. (1981) *Z. Naturforsch.* **36,** 988–996.
43. Hemker, M. B., Cheroutre, G., van Zwieten, R., Maaskant-van Wijk, P. A., Roos, D., Loos, J. A., van der Schoot, E. & von dem Borne, A. E. G. (2003) *Br. J. Haematol.* **122**, 333–340.
44. Birkenmeier, C. S., Gifford, E. J. & Barker, J. E. (2003) *Hematol. J.* **4,** 445–449.
45. Wandersee, N. J., Birkenmeier, C. S., Gifford, E. J., Mohandas, N. & Barker, J. E. (2000) *Hematol. J.* **1,** 235–242.
46. Yang, B., Ma, T. & Verkman, A. S. (2001) *J. Biol. Chem.* **276,** 624–628.
47. Avent, N. D., Liu, W., Warner, K. M., Mawy, W. J., Jones, J. W., Ridgwell, K. & Tanner, M. J. A. (1996) *J. Biol. Chem.* **271,** 14233–14239.
48. Soupene, E., Inwood, W. & Kustu, S. (2004) *Proc. Natl. Acad. Sci. USA* **101,** 7787–7792.
49. Cooper, G. J., Zhou, Y., Bouyer, P., Grichtchenko, I. I. & Boron, W. (2002) *J. Physiol. (Paris)* **542,** 17–29.
50. Fang, W., Yang, B., Matthay, M. A. & Verkman, A. S. (2002) *J. Physiol. (Paris)* **542,** 63–69.
51. Prasad, G. V., Coury, L. A., Finn, F. & Zeidel, M. L. (1998) *J. Biol. Chem.* **273,** 33123–33126.
52. Uehlein, N., Lovisolo, C., Siefritz, F. & Kaldenhoff, R. (2003) *Nature* **425,** 734–737.
53. Khademi, S., O'Connel, J., Remis, J., Robles-Colmenares, Y., Miercke, L. J. W. & Stroud, R. M. (2004) *Science* **305,** 1587–1594.
53. Frank, A. E. & Weiner, I. D. (2001) *J. Am. Soc. Nephrol.* **12,** 1607–1614.
55. Chernova, M. N., Stewart, A. K., Jiang, L., Friedman, D. L., Kunes, Y. Z. & Alper, S. L. (2003) *Am. J. Physiol. Cell Physiol.* **284,** C1235–C1246.
56. Javelle, A., Severi, E., Thornton, J. & Merrick, M. (2004) *J. Biol. Chem.* **279,** 8530–8538.